Journal of Lasers in Medical Sciences

J Lasers Med Sci. 2025;16:e26

Original Article

http://journals.sbmu.ac.ir/jlms

doi 10.34172/jlms.2025.26

Transscleral Photodynamic Therapy with a Chlorin e6 Photosensitizer in a Rabbit Experimental Model of an Intraocular Mass Lesion

Ernest V. Boiko[1,2,3], Elena V. Samkovich[1*], Irina E. Panova[1,2,3], Sergey B. Shevchenko[4], Sergey L. Vorobyev[5], Elizaveta S. Kalashnikova[5], Elizaveta A. Masian[1], Victoria G. Gvazava[1]

[1]Department of Scientific and Education,Fyodorov "Eye Microsurgery" Federal State Institution, St. Petersburg Branch, Saint Petersburg, Russian Federation
[2]Department of Ophthalmology, Federal State Budgetary Educational Institution of Higher Professional Education "North-Western State Medical University named after I.I. Mechnikov," Saint Petersburg, Russian Federation
[3]Medical Faculty, Department of Ophthalmology, Federal State Budgetary Educational Institution of Higher Professional Education "Saint Petersburg State University," Saint Petersburg, Russian Federation
[4]Department of Physiology of Visceral Systems, Federal State Budgetary Scientific Institution "Institute of Experimental Medicine," Saint Petersburg, Russian Federation
[5]National Center for Clinical Morphological Diagnostics, Saint Petersburg, Russian Federation

***Correspondence to**
Elena V. Samkovich,
Email: e.samkovich@mail.ru

Received: March 26, 2025
Accepted: May 31, 2025
ePublished: August 20, 2025

Abstract

Introduction: In vivo modeling of intraocular neoplasms remains challenging due to the limitations of conventional methods, such as the poor viability of xenografted B16 melanoma cells, the need for immunosuppression, and discrepancies between histopathological features and those of human uveal melanoma. Developing a biologically relevant, reproducible model for transscleral photodynamic therapy (TS-PDT) using chlorin-based photosensitizers is essential, particularly to assess radiation penetration depth and the safety profile of the method.

Methods: A model of an intraocular mass was created using an alloplant—an acellular biomaterial derived from the kidney capsule—implanted into the suprachoroidal space of rabbit eyes in both pigmented and non-pigmented variants. TS-PDT was performed using chlorin e6 (2.5 mg/kg) and a 660 nm laser (0.17 W, 10 minutes). Monitoring included ultrasound imaging, fundus photography, and histological analysis conducted 41 days post-treatment.

Results: The alloplant maintained structural integrity and elicited only minimal inflammatory response. The absence of thermal damage to the sclera confirmed the safety of the selected treatment parameters. In the choroid, focal thrombosis, vascular ectasia, and stromal fibrosis were observed. Retinal necrosis overlying the alloplant (penetration depth > 3 mm) indicated sufficient radiation penetration. The pigmented model demonstrated accumulations of pigment-laden macrophages, replicating the optical properties of melanin-containing tissues.

Conclusion: This alloplant-based model enables standardized TS-PDT investigation with clinical relevance and confirmed safety. The selective effect on deep ocular tissues supports TS-PDT's potential in eye-preserving tumor therapy. Future directions include studying neovascularization and optimizing treatment protocols.

Keywords: Transscleral photodynamic therapy; Uveal melanoma; Photosensitizer; Intraocular tumor; Ocular oncology.

Introduction

The in vivo modeling of tumor processes is a key tool in preclinical research, enabling the investigation of therapeutic responses in oncology.[1,2] In the field of ocular oncology, the development of models simulating intraocular mass lesions holds particular significance, as it allows for the replication of the spatial, biological, and biomechanical characteristics of pathological formations, including tumors of the uveal tract.[3-5] For the investigation of laser-based therapeutic modalities, it is essential to employ a model in which the characteristics of the neoplasm—such as localization, thickness, volume, and pigmentation—can be precisely controlled under in vivo conditions. These parameters are critical for establishing defined optical environments in terms of transmission, absorption, and scattering within biological tissues. It should be noted that models based on xenotransplantation of tumor cell lines into the ocular coats, such as B16 melanoma, are associated with several methodological limitations.[3,6] The low survival rate of this cell line (less than 30% without

Please cite this article as follows: Boiko EV, Samkovich EV, Panova IE, Shevchenko SB, Vorobyev SL, Kalashnikova ES, et al. Transscleral photodynamic therapy with a chlorin e6 photosensitizer in a rabbit experimental model of an intraocular mass lesion. *J Lasers Med Sci.* 2025;16:e26. doi:10.34172/jlms.2025.26.

immunosuppression) complicates the establishment of a stable model and necessitates repeated attempts, thereby increasing both time and resource expenditures.[4] Sustaining the viability of B16 melanoma cells requires prolonged immunosuppression in experimental animals, which further complicates study implementation and increases associated costs.[7,8] Moreover, the aggressive growth and atypical vascularization of B16 melanoma do not fully correspond to the histopathological and hemodynamic characteristics of human uveal melanoma, thereby reducing the predictive value of such models.[7,9] Photodynamic therapy (PDT) in ocular oncology is traditionally performed via a transpupillary approach, as documented in numerous studies.[10-13] The transscleral approach, however, offers distinct advantages, particularly for accessing tumors located in peripheral regions. Existing in vivo studies on PDT have either focused on transpupillary techniques or utilized models that did not evaluate the optical properties of the sclera, creating a gap in the assessment of the safety and efficacy of the transscleral approach.[14,15] Previous investigations into transscleral therapeutic modalities, including those by Boiko et al,[16] laid the foundation for understanding laser exposure parameters in thermotherapy and substantiated the rationale for employing the transscleral route in PDT. In ex vivo experiments utilizing sclera–choroid bovine tissue models, it was demonstrated that transscleral thermotherapy using 0.81 μm wavelength radiation achieved coagulation in tissues up to 4 mm thick, while maintaining scleral integrity under optimized power settings (0.5–1.0 W) and exposure durations (15–60 seconds).[16] These findings underscore the feasibility and importance of precise control over energy parameters to minimize the risk of thermal damage—an especially pertinent consideration in PDT. Nevertheless, such ex vivo sclera–choroid models do not account for the dynamic biological processes that are pivotal in PDT.

Transscleral photodynamic therapy (TS-PDT) using chlorin-based photosensitizers, which involves the delivery of laser radiation through the sclera, requires a detailed investigation of light–tissue interactions, particularly with respect to penetration depth. Chlorin E6 is a potent photosensitizer and the active component of several drugs, including Fotolon, Fotoditazin, and Fotoran. Chlorin E6-based drugs were developed and approved in Belarus for clinical use in 2001, followed by approval in Russia in 2004 (Instructions for the use of the medicinal product Fotoran E6 [lyophilizate for preparation of infusion solution]. Registration certificate LP-004885 dated June 13, 2018 [in Russian][17]). However, no existing models allow for the assessment of these parameters under conditions that approximate clinical scenarios. To study the effects of TS-PDT on deeper ocular tissues, the use of an alloplant—an acellular biomaterial derived from the fibrous capsule of the kidney—may serve as an appropriate model for simulating an intraocular mass. Its layered structure, primarily composed of type I collagen, provides mechanical stability, while the absence of antigens minimizes immune response, thereby enabling the creation of a controllable and reproducible model.[18] One of the principal advantages of the proposed method is its relative technical simplicity, which facilitates implementation and reduces associated costs.

A key benefit of the alloplant model is its capacity for modification, including the addition of pigment to replicate the optical properties of melanin-containing tissues. This feature makes it particularly suitable for studying laser–tissue interactions in the context of TS-PDT—a therapeutic modality that has not previously been investigated using such models. Additionally, the use of the alloplant-based biomaterial enables the evaluation of the penetrating capacity of laser radiation through the scleral shell of the eyeball.

The aim of this study was to develop an experimental model of an intraocular mass lesion for the investigation of the safety, penetration depth, and biological effects of TS-PDT using a chlorin e6 photosensitizer.

Materials and Methods

The experimental study was conducted on a single rabbit of the Soviet Chinchilla breed, weighing 3.0 kg. The animal was housed under standard vivarium conditions with controlled light-dark cycles (12/12 hours), ambient temperature (22 ± 2 °C), and relative humidity (50 ± 10%), with unrestricted access to water and a specialized diet. The study was conducted in accordance with the principles of the Declaration of Helsinki and the European Directive 2010/63/EU on the protection of animals used for scientific purposes. The experimental protocol was approved by the Local Ethics Committee of the Federal State Budgetary Scientific Institution "Institute of Experimental Medicine" (Protocol No. 4/24 dated 24 October 2024).

Prior to inclusion in the study, the rabbit underwent a comprehensive ophthalmological examination to exclude any comorbid pathologies. Only animals with intact optical media and without signs of inflammation, hemorrhage, or developmental anomalies were eligible for further procedures.

General anesthesia was induced via intramuscular injection of 1 mL Zoletil (tiletamine–zolazepam, 50 mg/mL) and 0.3 mL Rometar (medetomidine, 20 mg/mL). The modeling procedure was performed on both eyes.

To simulate an intraocular mass lesion, an alloplant derived from the fibrous capsule of the kidney was used ("Alloplant for Conjunctival Plasty," Registration Certificate No. FSR 2011/12012, dated 29 December 2021; manufacturer: Federal State Budgetary Institution "All-Russian Center for Eye and Plastic Surgery," Ministry of Health of the Russian Federation, Ufa). Histologically, this biomaterial consists of densely packed type I

collagen fibers arranged in a lamellar structure, providing mechanical stability and minimizing deformation during implantation. The alloplant's biological properties are characterized by high biocompatibility due to the absence of active stromal, epithelial, and lymphoid cells, as well as antigenic determinants, thereby minimizing the immune response.[18] For the creation of a pigmented variant of the model, the alloplant was pre-incubated in a solution of black fabric dye.

The modeling procedure involved the implantation of the alloplant into the suprachoroidal space of the rabbit's eyeball. Surgical access was obtained in the equatorial zone of the eye. After fixation of the extraocular muscles, a full-thickness scleral incision was made to create a pocket in the suprachoroidal space. The alloplant was implanted into the pocket (non-pigmented in the right eye, pigmented in the left eye). The correct positioning of the implant was verified intraoperatively using a wide-angle ophthalmic lens under pharmacologically induced mydriasis. The scleral and conjunctival incisions were closed with interrupted sutures (Vicryl 8-0). Following implantation into both eyes, the accuracy of model formation was verified.

Throughout all stages of the study, the following diagnostic methods were employed: ultrasonography with color Doppler imaging (CDI) using a PHILIPS Affinity 50 system equipped with a linear transducer (L15-7io, 15–7 MHz) in B-mode and CDI mode. This enabled confirmation of the alloplant's localization, dimensions, and the presence or absence of vascularization, based on the detection of color-coded flow signals. In addition, fundus photography was performed using the ZEISS CLARUS 500 camera. Imaging was conducted under mydriasis to evaluate the topographic correlation of the model with clinical characteristics of uveal melanoma and to exclude any iatrogenic injury. TS-PDT was initiated only after successful verification of model formation.

Two hours after the modeling of the intraocular mass lesion, TS-PDT was performed using the laser system "ALOD-01" (Alkom Medica, Russia, Registration number: No. FSR 2011/10343) in combination with the photosensitizer chlorin e6 ("Fotoran" 2.5 mg/kg), administered as a single intravenous bolus 30 minutes prior to laser exposure. A transscleral probe with a diameter of 5 mm and an integrated thermosensor was used to deliver laser radiation and to enable continuous monitoring of the scleral temperature.[19,20] Prior to the treatment, laser power output was verified using a dosimeter to ensure compliance with the preset parameters displayed on the laser device. During irradiation, continuous temperature monitoring was performed with real-time data recording at baseline, 5 minutes, and 10 minutes. The parameters of photodynamic therapy and the thermometric data for each eye are presented in Table 1.

Table 1. Parameters of Transscleral Photodynamic Therapy for the Right (Non-Pigmented Model) and Left (Pigmented Model) Eyes of the Rabbit

Parameter	Right Eye (Non-pigmented Model)	Left Eye (Pigmented Model)
Probe diameter	5 mm	5 mm
Laser power	0.17 W	0.17 W
Power density	0.866 W/sm^2	0.866 W/sm^2
Energy density	519.48 J/cm^2	519.48 J/cm^2
Exposure time	10 min	10 min
Temperature (start /5 min/10 min)	28°C/32°C/37°C	28°C/33°C/38°C

Results

Postoperative monitoring was performed at 1 day, 1 week, 2 weeks, and 1 month following TS-PDT. According to ultrasonography of the rabbit's right eye (non-pigmented model), conducted in B-mode 40 days after modeling of the intraocular mass lesion, a protruding intraocular hyperechoic focus with homogeneous echogenicity was identified, measuring up to 4.6 mm in height and up to 2.9 mm in base diameter. CDI revealed color flow signals within the projection of the formed lesion (Figure 1A, B).

Ultrasound examination of the left eye (pigmented model), performed 40 days post-modeling, revealed a protruding intraocular hyperechoic focus with homogeneous echogenicity in the mid-peripheral zone, measuring up to 2.8 mm in height and up to 4.1 mm in base diameter. CDI demonstrated color flow along the peripheral margins of the alloplant (Figure 1C, D).

Fundus photography of the right eye (non-pigmented model) showed a volumetric lesion located in the superior mid-peripheral quadrant, measuring approximately 3 PD (pupil diameters) (Figure 2A).

Fundus photography of the left eye (pigmented model) revealed a pigmented volumetric lesion in the inferior mid-peripheral quadrant, also measuring approximately 3 PD (Figure 2B).

To assess histopathological outcomes, we performed enucleation followed by histological examination 41 days after TS-PDT. The results of the histological analysis of the enucleated rabbit eyes are summarized in Table 2.

Histological Findings in the Intraocular Mass Model of the Rabbit's Right Eye (Non-Pigmented Model)

In the right eye, an allotransplant (fibrous kidney capsule) was identified between the choroid and sclera. The implant was characterized by sparse clusters of macrophages and multinucleated giant cells of the foreign body type, mild and uneven vascularization, and minimal focal lymphohistiocytic inflammatory infiltration (Figure 3A–D). The sclera exhibited no signs of thermal damage (no evidence of coagulation or deformation) and was composed of uniformly thick collagen fibers and monomorphic fibrocytes (Figure 4A). The choroid demonstrated focal vascular ectasia, focal thrombosis,

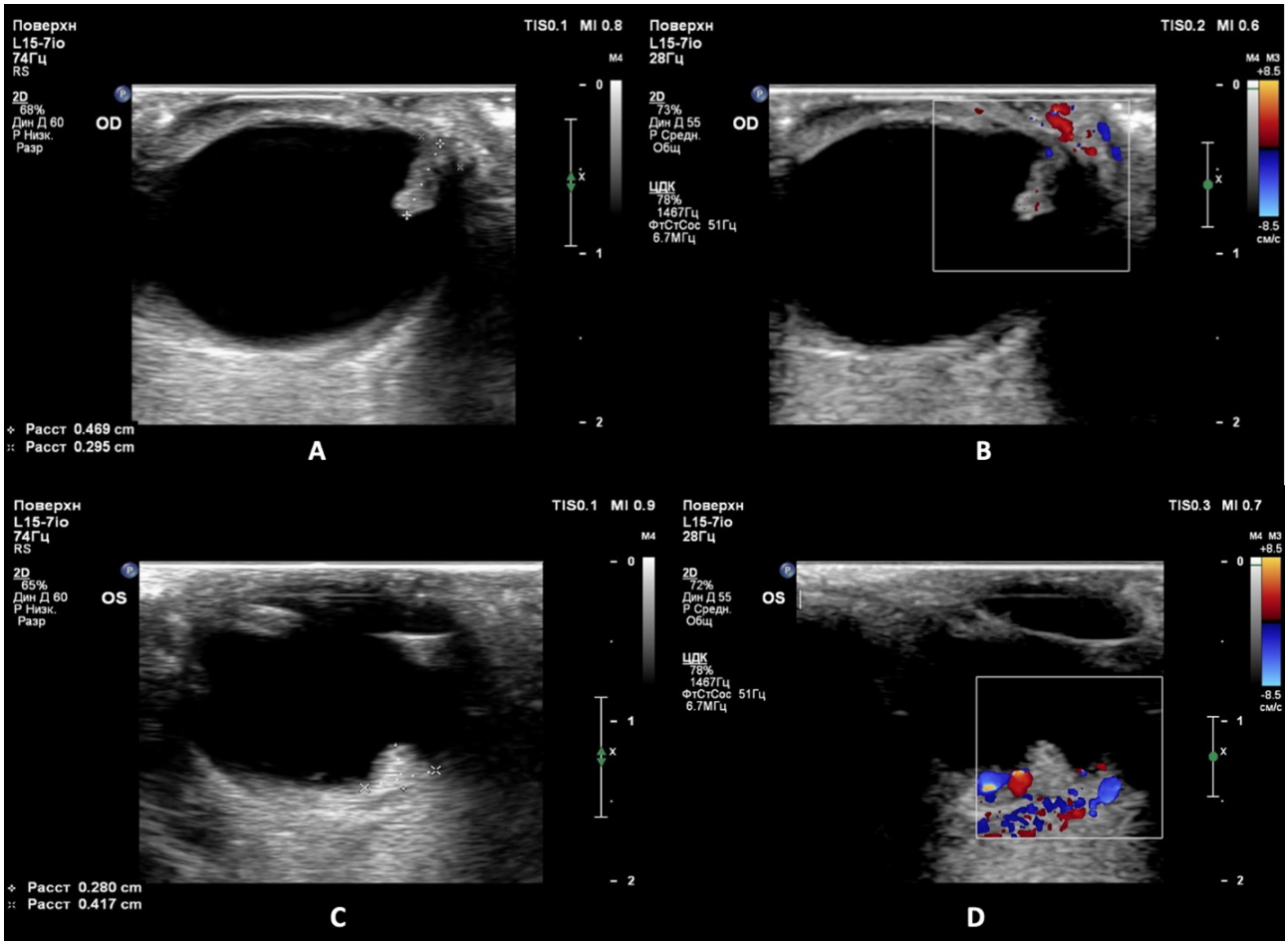

Figure 1. A – B-mode ultrasonography of the rabbit's right eye (non-pigmented model): in the upper part of the image, a modeled intraocular mass lesion without pigment is visible, measuring 4.6 mm in height and up to 2.9 mm in base diameter. B – CDI mode of the same eye: color flow signals within the lesion projection. C – B-mode ultrasonography of the rabbit's left eye (pigmented model): in the lower part of the image, a pigmented intraocular mass lesion is visible, measuring up to 2.8 mm in height and 4.1 mm in base diameter. D – CDI mode of the left eye: color flow detected along the peripheral margins of the alloplant

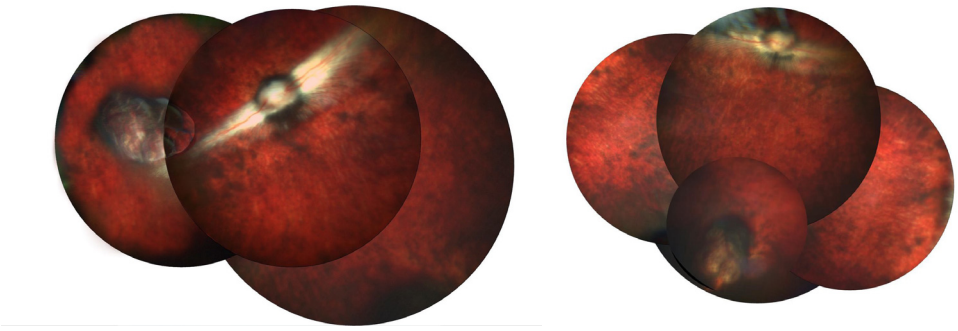

Figure 2. A – Fundus image of the rabbit's right eye (non-pigmented model) after modeling of the intraocular mass lesion. B – Fundus image of the left eye (pigmented model) after modeling of the intraocular mass lesion

vascular paresis, and vascular congestion with erythrocyte microthrombi. Additionally, stromal fibrosis, vascular engorgement, and minimal lymphocytic infiltration were observed, accompanied by choroidal edema both within the projection of the alloplant and in the laser-irradiated zone outside the alloplant (Figure 4A–E). The retina exhibited aseptic necrotic changes both overlying the alloplant and within the area of photodynamic exposure beyond its borders (Figure 5A–D).

Histological Findings in the Intraocular Mass Model of the Rabbit's Left Eye (Pigmented Model)

In the left eye, an allotransplant (fibrous kidney capsule) was similarly positioned between the choroid and sclera. Histological analysis revealed isolated macrophages and multinucleated giant cells of the foreign body type, focal vascularization, and minimal lymphohistiocytic inflammatory infiltration (Figure 6A–C). Within the alloplant, clusters of pigmented macrophages were

Table 2. Histological Analysis of Rabbit Eyeballs in Intraocular Mass Models Following Transscleral Photodynamic Therapy

Criterion	Non-Pigmented Model (5 mm Transscleral Probe)	Pigmented Model (5 mm Transscleral Probe)
Sclera		
Thermal damage	Absent (uniform fibers, monomorphic rare fibrocytes)	Absent (uniform fibers, monomorphic rare fibrocytes)
Choroid		
Vascular ectasia	Focal	Focal
Thrombosis	Focal thromboses, erythrocyte thrombi	Focal thromboses, erythrocyte thrombi
Vascular paresis	Present	Present
Stromal fibrosis	Marked	Marked
Edema	Present (within alloplant projection and adjacent irradiated areas)	Present (within alloplant projection and adjacent irradiated areas)
Retina		
Necrotic, aseptic changes	Overlying the alloplant and in irradiated zones beyond it	Overlying the alloplant and in irradiated zones beyond it
Alloplant		
Macrophages/multinucleated giant cells	Few clusters of macrophages and multinucleated giant cells of "foreign body" type	Scattered macrophages and multinucleated giant cells of the foreign body type
Vascularization	Minimal	Focal
Inflammation	Minimal focal lymphohistiocytic infiltration	Minimal focal lymphohistiocytic infiltration
Pigmentation	Absent	Clusters of pigmented macrophages

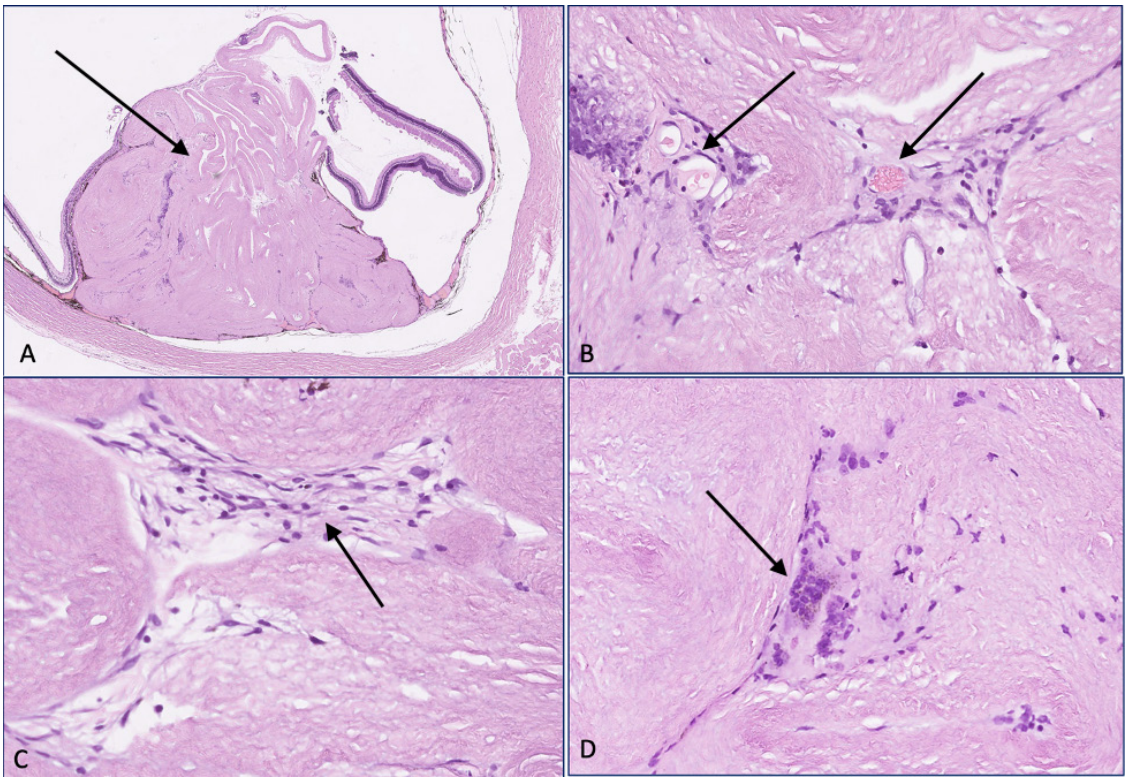

Figure 3. A – Modeling of the intraocular mass lesion. Non-pigmented alloplant (arrow), ×40, H&E. B – Vascularization of the alloplant (arrow), ×400, H&E. C – Minimal lymphoid infiltration in the alloplant (arrow), ×200, H&E. D – Macrophages and multinucleated giant cells of the foreign body type within the alloplant (arrow), ×100, H&E

also identified (Figure 6D). The sclera showed no signs of thermal damage (no evidence of coagulation or deformation) and was composed of uniformly thick collagen fibers and monomorphic fibrocytes (Figure 4A). The choroid exhibited focal vascular ectasia, focal thrombosis, vascular paresis, and congestion with erythrocyte microthrombi. Irregular stromal fibrosis, vascular congestion, and minimal lymphocytic infiltration were also noted, accompanied by choroidal edema both within the region of the alloplant and in the

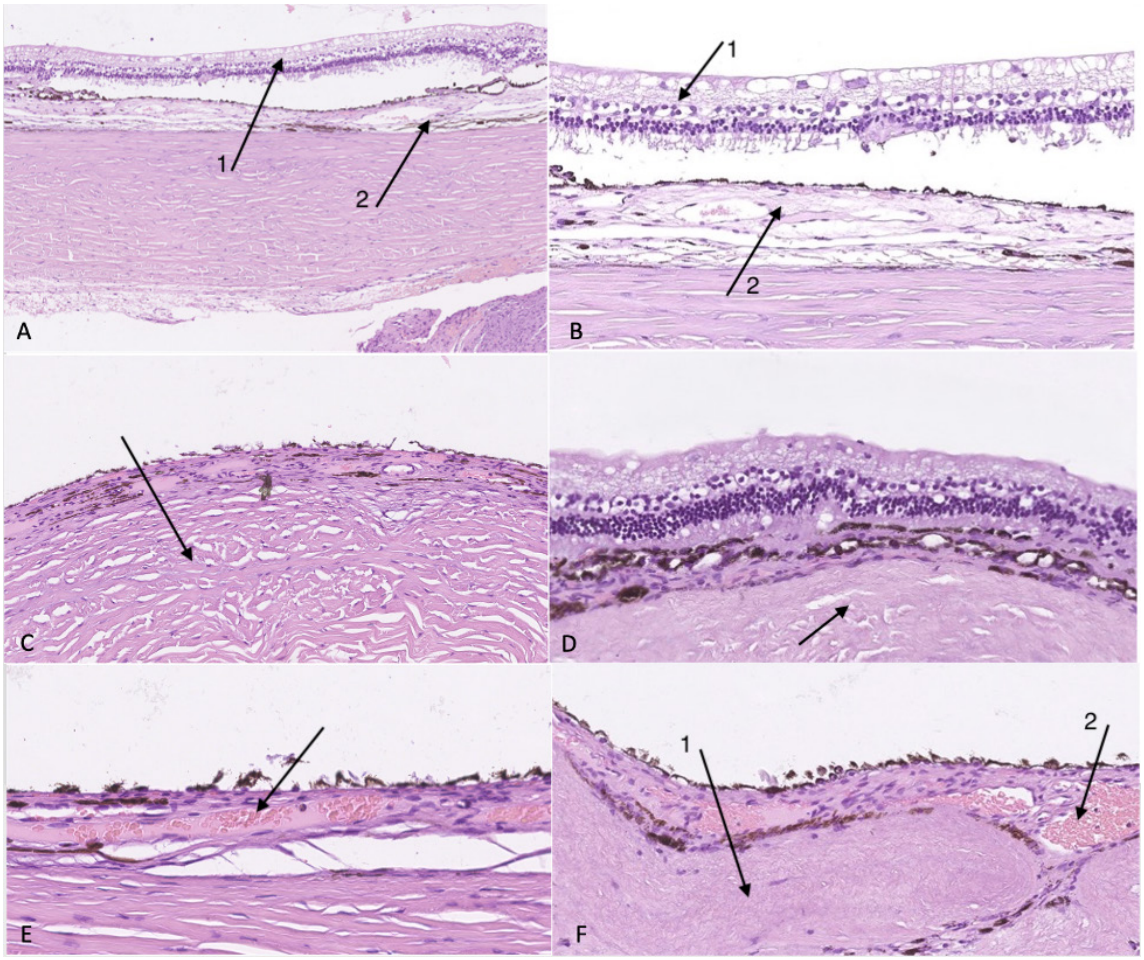

Figure 4. A – Intact sclera, choroidal edema (arrow 2) outside the alloplant. Mild polymorphism (arrow 1) of retinal epithelium in the TS-PDT zone, ×100, H&E. B – Choroidal edema (arrow 2) and retinal epithelial polymorphism (arrow 1) in the irradiation zone outside the alloplant, ×400, H&E.C – Choroidal stromal fibrosis in the irradiated zone outside the alloplant (arrow), ×200, H&E. D – Choroidal fibrosis in the alloplant zone (arrow), ×200, H&E. E – Vascular paresis and congestion with erythrocyte thrombi (arrow), ×200, H&E. F – Choroidal fibrosis (arrow 1) and vascular paresis with erythrocyte thrombi (arrow 2), ×200, H&E

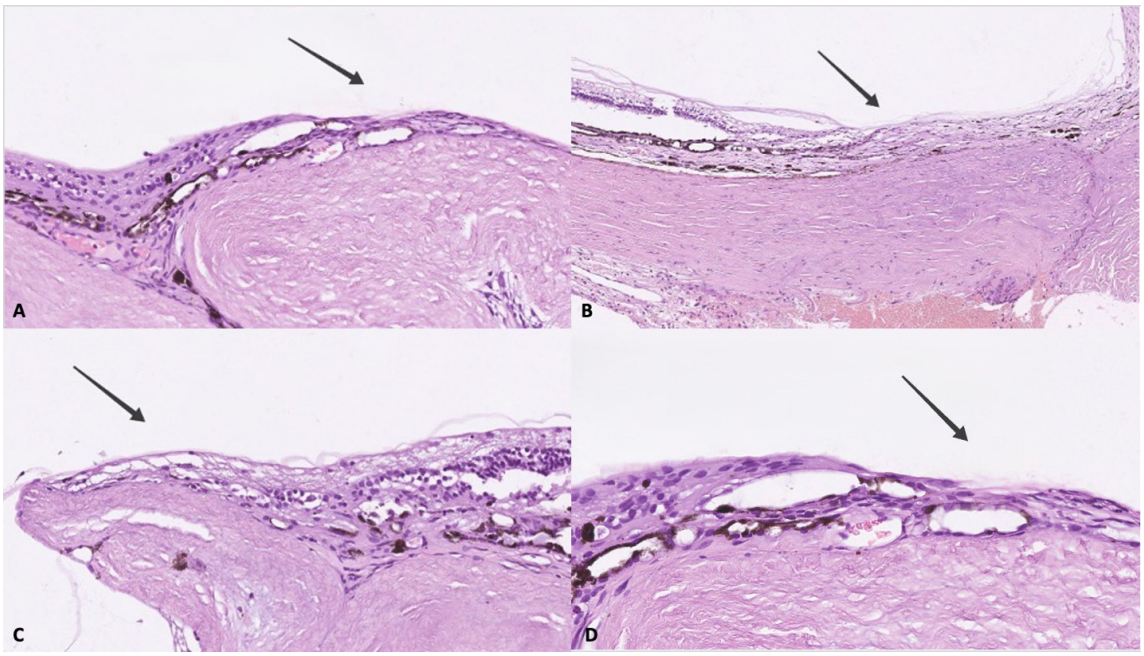

Figure 5. A – Aseptic retinal necrosis overlying the alloplant (arrow), ×200, H&E. B – Retinal necrosis in the irradiated zone outside the alloplant (arrow), ×200, H&E. C – Retinal necrosis overlying the alloplant (arrow), ×200, H&E. D – Retinal necrosis overlying the alloplant (arrow), ×400, H&E

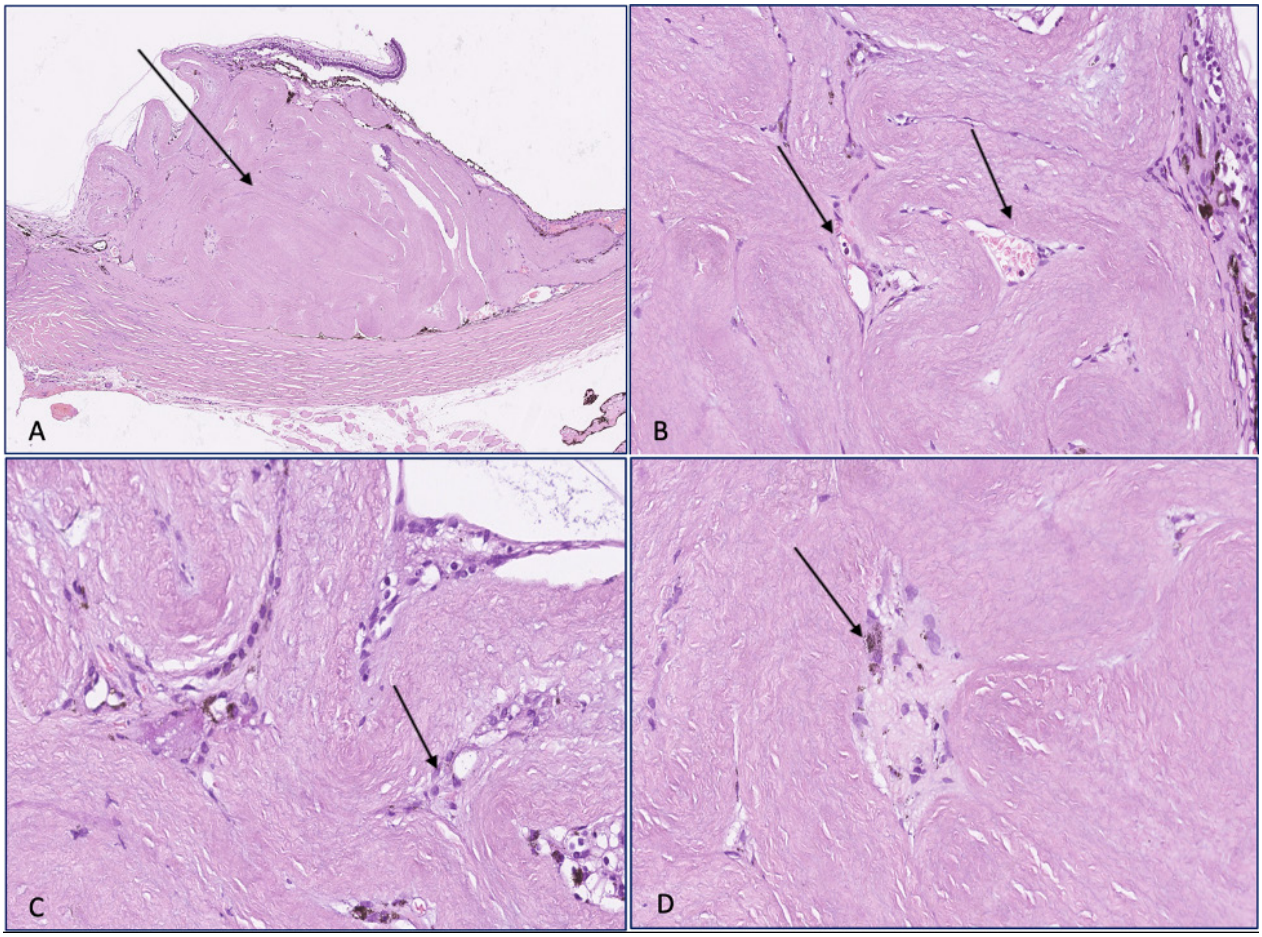

Figure 6. A – Modeling of the intraocular mass lesion. Pigmented alloplant (arrow), ×40, H&E. B – Vascularization of the alloplant (arrow), ×200, H&E. C – Minimal inflammation within the alloplant (arrow), ×400, H&E. D – Cluster of multinucleated macrophages with pigmented cytoplasm (arrow), ×400, H&E

laser-irradiated area outside the implant (Figure 4A–E). The retina demonstrated necrotic changes overlying the alloplant as well as within the zone of photodynamic exposure beyond it (Figure 5A–D).

Discussion

TS-PDT, utilizing a 660 nm wavelength laser in combination with a chlorin-based photosensitizer, represents an innovative approach to the treatment of intraocular tumors. A key advantage of this method lies in the ability of laser radiation to traverse the scleral shell with minimal energy loss, enabling selective targeting of tissues at the base of the pathological lesion. This effect is facilitated by the optical properties of the sclera and choroid, which support uniform energy distribution in deeper layers while minimizing the risk of thermal damage to superficial structures.

The developed intraocular mass model, based on the implantation of an alloplant (fibrous kidney capsule), overcomes the limitations and complexities of traditional approaches used to simulate volumetric pathological processes within the eye. The pigmented variant of the model replicates the optical properties of melanin-containing tissues, thereby enhancing its clinical relevance. Implantation of the alloplant into the suprachoroidal space of the rabbit eye is particularly justified, given that the optical and thermal properties of rabbit sclera closely resemble those of human sclera, ensuring translational applicability.[15,21]

The present study demonstrates that TS-PDT with chlorin e6 induces specific alterations in ocular tissues that simulate intraocular tumors. The sclera remained intact in both models, showing no evidence of coagulation or collagen fiber deformation, thereby confirming the safety of the selected TS-PDT parameters (laser power: 0.17 W; exposure time: 10 minutes). The absence of thermal damage, even after extended irradiation, is consistent with literature data indicating that temperatures below 40 °C do not induce coagulative necrosis.

In the choroid, focal vascular disturbances—including ectasia, microthrombosis, and stromal fibrosis—were observed, reflecting the direct impact of photooxidative reactions on vascular endothelium, in line with the known mechanisms of PDT. Notably, these effects were localized, likely due to the structural integrity of physiologically normal choroidal vessels. In contrast, intratumoral vessels—characterized by endothelial discontinuities such as slit-like lumens and absence of basement membranes—

are more vulnerable to PDT. Photosensitizer accumulation in these abnormal vessels amplifies oxidative stress, leading to endothelial dysfunction and intravascular thrombosis.[12,22]

Necrotic changes in the retina overlying the modeled intraocular lesion at a depth exceeding 3 mm from the scleral surface may be attributable to either mechanical trauma during surgical intervention or to photochemical reactions induced by TS-PDT. The presence of necrosis in peripheral retinal zones beyond the implant site supports the latter hypothesis, suggesting that the laser radiation effectively penetrated into therapeutically meaningful depths consistent with intraocular tumor treatment.

The alloplant preserved its structural integrity and elicited only minimal focal inflammatory responses. However, at 41 days post-intervention, histological analysis revealed focal neovascularization within the implant. These findings were corroborated by Doppler ultrasonography, which detected color flow signals correlating with histologically confirmed neovessel formation. This phenomenon likely reflects tissue remodeling, consistent with prior studies employing vascularized sponge allografts.[18,23] The ability of the alloplant to simulate neovascularization presents an opportunity to investigate photosensitizer behavior in areas of increased metabolic activity. A promising direction for future research is to perform TS-PDT during the delayed phase, following the formation of a mature neovascular network within the alloplant, to evaluate thrombotic responses under conditions closely approximating clinical pathology. The use of alternative biomaterials — such as choroid, muscle, or conjunctiva — could further enhance the biological relevance of the model.

The depth of PDT penetration remains a topic of ongoing investigation. In the present study, the chlorin e6 photosensitizer, activated at 660 nm, achieved clinically meaningful effects at tissue depths of 3–4 mm. In comparison, first-generation photosensitizers such as hematoporphyrin (630 nm) and 5-aminolevulinic acid (375–440 nm) are limited to penetration depths of 1–3 mm due to pronounced light absorption and scattering in superficial layers.[24] Chlorins offer a distinct advantage due to their optimized absorption spectra in the near-infrared range (660 nm), resulting in reduced energy losses and enabling radiation penetration of up to 3–4 mm in this experiment and up to 4–6 mm according to literature data.[10,25,26] This benefit is attributable to the reduced interaction of long-wavelength light with melanin and hemoglobin—an especially important factor in the treatment of pigmented intraocular tumors such as uveal melanoma (UM). In this study, effective penetration was supported by histologically verified aseptic retinal necrosis overlying the alloplant, consistent with therapeutic thresholds for small- to medium-sized tumors.[27]

Nevertheless, for tumors exceeding 3 mm in thickness, PDT efficacy may decrease due to progressive attenuation of light by tissue absorption and scattering, warranting further optimization of treatment protocols. Importantly, even with prolonged exposure (10 minutes) and high energy density (519.48 J/cm^2), no thermal damage to the sclera was observed, affirming the safety of the technique. These findings underscore the potential of TS-PDT as an organ-preserving treatment modality for intraocular tumors, where achieving sufficient tissue penetration without compromising structural integrity is crucial.

Pigmentation—particularly in intraocular tumors such as UM—has traditionally limited PDT efficacy due to melanin's high absorption properties and its ability to neutralize reactive oxygen species.[28,29] However, recent advances using chlorin-based photosensitizers activated in the near-infrared spectrum have opened new therapeutic possibilities. In this spectral range, melanin absorption is significantly reduced, permitting light penetration to depths of 4–6 mm, as shown in preclinical studies.[10,25]

To better simulate clinical conditions, standardization of pigmentation levels is essential. This can be achieved by incubating the alloplant in solutions of melanin analogs or biological dyes with controlled concentrations. Pigmentation can be quantitatively and qualitatively assessed using spectrophotometry in the 600–900 nm range and by histological staining. Additional strategies to overcome optical barriers include the use of optical clearing agents—such as polyethylene glycol—which reduce light scattering by equalizing the refractive index of tissues, thereby enhancing penetration depth by 30–50%.[30,31] Future developments may include the creation of photosensitizers activated in the 700–900 nm range, where melanin absorption is minimal, as well as the use of nanoparticle-based carriers for targeted delivery. Such innovations hold promise for overcoming the limitations imposed by high pigmentation.[32,33] Standardization of experimental models and the adaptation of therapeutic protocols to tissue optical properties will not only improve preclinical reproducibility but also enhance clinical applicability, enabling organ-preserving treatment even in challenging cases of pigmented tumors.

Study Limitations

This study has several limitations. First, the use of a single animal limits statistical power and generalizability, underscoring the need for larger sample sizes in future investigations. Second, the acellular nature of the alloplant precludes the evaluation of cell-mediated immune responses. Third, the model incorporated only two levels of pigmentation; a graded approach (e.g., low, moderate, high pigmentation) would better reflect the clinical heterogeneity of uveal melanoma. Finally, the absence of pre-existing vasculature in the model limits its capacity to evaluate angiogenesis and vascular response to therapy, necessitating further model refinement for in vivo studies of neovascularization.

Conclusion

1. The developed alloplant-based model effectively simulates intraocular mass lesions, including pigmented variants, and provides standardized conditions for investigating laser–tissue interactions within the eyeball.
2. The absence of thermal damage to the sclera confirms the safety of the selected laser parameters and the design of the transscleral probe.
3. The selective action of TS-PDT is evidenced by focal microthrombosis, vascular ectasia, and stromal fibrosis in the choroid, indicating targeted endothelial injury mediated by photooxidative reactions.
4. TS-PDT achieves sufficient penetration depth of laser radiation (>3 mm), as demonstrated by aseptic necrotic changes in the retina overlying the alloplant.

Final Remarks

This study substantially enhances the preclinical assessment of TS-PDT by introducing a cost-effective and biologically relevant experimental model. A promising direction for future research involves performing TS-PDT during the delayed phase following the development of a mature neovascular network within the alloplant or alternative biomaterials. This would enable the evaluation of thrombotic effects under conditions that closely replicate clinical settings. The findings provide a foundation for the development of organ-preserving therapeutic protocols for patients with intraocular tumors, offering a combination of high therapeutic efficacy and minimal invasiveness.

Authors' Contribution

Conceptualization: Ernest V. Boiko, Irina E. Panova, Elena V. Samkovich.
Formal analysis: Elena V. Samkovich, Sergey B. Shevchenko, Elizaveta S. Kalashnikova.
Investigation: Elena V. Samkovich, Elizaveta A. Masian, Victoria G. Gvazava.
Methodology: Ernest V. Boiko, Irina E. Panova, Elena V. Samkovich.
Project administration: Ernest V. Boiko, Sergey B. Shevchenko, Sergey L. Vorobyev.
Resources: Ernest V. Boiko, Elena V. Samkovich, Sergey B. Shevchenko, Sergey L. Vorobyev.
Supervision: Ernest V. Boiko, Irina E. Panova.
Validation: Ernest V. Boiko, Irina E. Panova, Elena V. Samkovich, Sergey B. Shevchenko, Sergey L. Vorobyev.
Visualization: Elena V. Samkovich, Elizaveta S. Kalashnikova, Elizaveta A. Masian, Victoria G. Gvazava.
Writing–original draft: Ernest V. Boiko, Irina E. Panova, Elena V. Samkovich, Sergey L. Vorobyev, Elizaveta S. Kalashnikova, Elizaveta A. Masian, Victoria G. Gvazava.
Writing–review & editing: Ernest V. Boiko, Irina E. Panova, Elena V. Samkovich.

Competing Interests

None.

Ethical Approval

The study was conducted in accordance with the principles of the Declaration of Helsinki and the European Directive 2010/63/EU on the protection of animals used for scientific purposes. The experimental protocol was approved by the Local Ethics Committee of the Federal State Budgetary Scientific Institution "Institute of Experimental Medicine" (Protocol No. 4/24 dated 24 October 2024).

Funding

This study was supported by a grant from the Russian Science Foundation (Project No. 24-75-00047, https://rscf.ru/project/24-75-00047/.

References

1. Giacobbe A, Abate-Shen C. Modeling metastasis in mice: a closer look. Trends Cancer. 2021;7(10):916-29. doi: 10.1016/j.trecan.2021.06.010.
2. Connolly KA, Fitzgerald B, Damo M, Joshi NS. Novel mouse models for cancer immunology. Annu Rev Cancer Biol. 2022;6(1):269-91. doi: 10.1146/annurev-cancerbio-070620-105523.
3. Cao J, Jager MJ. Animal eye models for uveal melanoma. Ocul Oncol Pathol. 2015;1(3):141-50. doi: 10.1159/000370152.
4. Uner OE, Gandrakota N, Azarcon CP, Grossniklaus HE. Animal models of uveal melanoma. Ann Eye Sci. 2022;7:7. doi: 10.21037/aes-21-30.
5. Goldrick C, Palanga L, Tang B, Mealy G, Crown J, Horgan N, et al. Hindsight: review of preclinical disease models for the development of new treatments for uveal melanoma. J Cancer. 2021;12(15):4672-85. doi: 10.7150/jca.53954.
6. Diaz CE, Rusciano D, Dithmar S, Grossniklaus HE. B16LS9 melanoma cells spread to the liver from the murine ocular posterior compartment (PC). Curr Eye Res. 1999;18(2):125-9. doi: 10.1076/ceyr.18.2.125.5380.
7. Stei MM, Loeffler KU, Holz FG, Herwig MC. Animal models of uveal melanoma: methods, applicability, and limitations. Biomed Res Int. 2016;2016:4521807. doi: 10.1155/2016/4521807.
8. Ordoñez JL, Saornil MA, Domingo E, Blanco G, Dieboldy, Morilla-Grasa A, et al. The need for continuous immunosuppression with cyclosporin A to maintain an experimental model of uveal melanoma. Melanoma Res. 2002;12(5):441-7. doi: 10.1097/00008390-200209000-00005.
9. Rodriguez Vicente J, Vicente Ortega V, Garcia Serrano F, Garcia Rojo B. Ocular melanoma: an experimental model in New Zealand white rabbits. Melanoma Res. 1993;3(3):195-202.
10. Belyi YuA, Tereshchenko AV, Volodin PL, Kaplan MA. Photodynamic Therapy with Photoditazine Photosensitizer in Ophthalmology. Kaluga: S. Fyodorov Eye Microsurgery Federal State Institution; 2008. [Russian].
11. Naumenko LV. Five-year outcomes of combined treatment in patients with large choroidal melanoma. Zdravookhranenie (Minsk). 2021;8(893):68-76. [Russian].
12. Belyi YuA, Tereshchenko AV, Volodin PL. Morphological study of photodynamic effects with photosensitizer "Photoditazine" on the structure of choroidal melanoma. Vestn Orenburg State Univ. 2007;78:19-22. Available from: http://vestnik.osu.ru/doc/1033/article/4123/lang/0. Accessed January 7, 2023. [Russian].
13. Samkovich EV, Panova IE, Boiko EV, Svistunova EM, Bykhovskii AA. Photodynamic therapy in the combined treatment of choroidal melanoma. Oftal'mokhirurgiya. 2024;139(2):99-108. doi: 10.25276/0235-4160-2024-2-99-108. [Russian].
14. Takhchidi KhP, Belyi YuA, Tereshchenko AV. Experimental results of photodynamic therapy in ophthalmology using domestic chlorin-based photosensitizers. Oftal'mokhirurgiya. 2005(2):30-5. [Russian].

15. Gonzalez VH, Hu LK, Theodossiadis PG, Flotte TJ, Gragoudas ES, Young LH. Photodynamic therapy of pigmented choroidal melanomas. Invest Ophthalmol Vis Sci. 1995;36(5):871-8.
16. Boiko EV, Shishkin MM, Sukhoterina AN, Kulikov AN. Possibilities of diode-laser transscleral retinopexy (compared with cryopexy) in vitreoretinal surgery. Oftal'mokhirurgiya i Terapiya. 2001;1(1):47-52. [Russian].
17. Juzeniene A. Chlorin e6-based photosensitizers for photodynamic therapy and photodiagnosis. Photodiagnosis Photodyn Ther. 2009;6(2):94-6. doi: 10.1016/j.pdpdt.2009.06.001.
18. Muldashev ER, ed. Regenerative Medicine. Alloplant Biomaterials in Ophthalmic Surgery. Ufa: All-Russian Center for Eye and Plastic Surgery; 2014. p. 432. [Russian].
19. Boiko EV, Ivanov AA, Samkovich EV, Panova IE, Grishacheva TG. Transscleral probe-tip for photodynamic therapy of uveal melanoma localized in the pre-equatorial segment with a tumor base diameter of 7.1–10.0 mm. Patent RF No. 228371U1; 26.08.2024. Bull. No. 24. [Russian].
20. Boiko EV, Samkovich EV, Panova IE, Svistunova EM, Ivanov AA, Bikhovsky AA. Hybrid photodynamic therapy as a component of combined treatment of uveal melanoma (preliminary results). Ophthalmology in Russia. 2024;21(4):755-63. doi: 10.18008/1816-5095-2024-4-755-763. [Russian].
21. Kang SJ, Zhang Q, Patel SR, Berezovsky D, Yang H, Wang Y, et al. In vivo high-frequency contrast-enhanced ultrasonography of choroidal melanoma in rabbits: imaging features and histopathologic correlations. Br J Ophthalmol. 2013;97(7):929-33. doi: 10.1136/bjophthalmol-2013-303343.
22. Mazloumi M, Dalvin LA, Abtahi SH, Yavari N, Yaghy A, Mashayekhi A, et al. Photodynamic therapy in ocular oncology. J Ophthalmic Vis Res. 2020;15(4):547-58. doi: 10.18502/jovr.v15i4.7793.
23. Muldashev ER, Musina LA, Shangina OR. Morphological evaluation of spongy allotransplants for ophthalmic surgery. Prakt Med. 2017;2(9). [Russian].
24. Quirk BJ, Brandal G, Donlon S, Vera JC, Mang TS, Foy AB, et al. Photodynamic therapy (PDT) for malignant brain tumors--where do we stand? Photodiagnosis Photodyn Ther. 2015;12(3):530-44. doi: 10.1016/j.pdpdt.2015.04.009.
25. Ferreira J, Menezes PF, Sibata CH, Allison RR, Zucoloto S, Castro e Silva O Jr, et al. Can efficiency of the photosensitizer be predicted by its photostability in solution? Laser Phys. 2009;19(9):1932-8. doi: 10.1134/s1054660x09170071.
26. Mansuri P, Tabaie SM, Naderi MS, Kebriti K, Esmaeeli Djavid G, Shirkavand A. Systemic photodynamic therapy with chlorine e6 as a photosensitizer for the treatment of nodular BCC: a case report. J Lasers Med Sci. 2022;13:e44. doi: 10.34172/jlms.2022.44.
27. Yordi S, Soto H, Bowen RC, Singh AD. Photodynamic therapy for choroidal melanoma: what is the response rate? Surv Ophthalmol. 2021;66(4):552-9. doi: 10.1016/j.survophthal.2020.09.006.
28. Vera RE, Lamberti MJ, Rivarola VA, Rumie Vittar NB. Developing strategies to predict photodynamic therapy outcome: the role of melanoma microenvironment. Tumour Biol. 2015;36(12):9127-36. doi: 10.1007/s13277-015-4059-x.
29. Li XY, Tan LC, Dong LW, Zhang WQ, Shen XX, Lu X, et al. Susceptibility and resistance mechanisms during photodynamic therapy of melanoma. Front Oncol. 2020;10:597. doi: 10.3389/fonc.2020.00597.
30. Pires L, Demidov V, Vitkin IA, Bagnato V, Kurachi C, Wilson BC. Optical clearing of melanoma in vivo: characterization by diffuse reflectance spectroscopy and optical coherence tomography. J Biomed Opt. 2016;21(8):081210. doi: 10.1117/1.Jbo.21.8.081210.
31. Pires L, Demidov V, Wilson BC, Salvio AG, Moriyama L, Bagnato VS, et al. Dual-agent photodynamic therapy with optical clearing eradicates pigmented melanoma in preclinical tumor models. Cancers (Basel). 2020;12(7):1956. doi: 10.3390/cancers12071956.
32. Lee SY, Lee R, Kim E, Lee S, Park YI. Near-infrared light-triggered photodynamic therapy and apoptosis using upconversion nanoparticles with dual photosensitizers. Front Bioeng Biotechnol. 2020;8:275. doi: 10.3389/fbioe.2020.00275.
33. Chen L, Chen M, Zhou Y, Ye C, Liu R. NIR photosensitizer for two-photon fluorescent imaging and photodynamic therapy of tumor. Front Chem. 2021;9:629062. doi: 10.3389/fchem.2021.629062.